

# Combined Differential and Common-Mode Scattering Parameters: Theory and Simulation

David E. Bockelman, *Member, IEEE*, and William R. Eisenstadt, *Senior Member, IEEE*

**Abstract**—A theory for combined differential and common-mode normalized power waves is developed in terms of even and odd mode impedances and propagation constants for a microwave coupled line system. These are related to even and odd-mode terminal currents and voltages. Generalized  $s$ -parameters of a two-port are developed for waves propagating in several coupled modes. The two-port  $s$ -parameters form a 4-by-4 matrix containing differential-mode, common-mode, and cross-mode  $s$ -parameters. A special case of the theory allows the use of uncoupled transmission lines to measure the coupled-mode waves. Simulations verify the concept of these mixed-mode  $s$ -parameters, and demonstrate conversion from mode to mode for asymmetric microwave structures.

## I. INTRODUCTION

THERE is an emerging need to measure RF and microwave differential circuits. Differential circuits have been important in communications systems for more than 50 years. Recent technological advances have pushed analog differential circuit performance limits into RF and low microwave frequencies.

Typically, differential circuits are designed and analyzed with traditional analog techniques, which employ lumped element assumptions. Examples of such analog differential circuit design and analysis are found in the texts by Gray and Meyer [1] and Middlebrook [2]. RF and microwave differential circuits contain distributed circuit elements, and require distributed circuit analysis and testing. Furthermore, traditional methods of testing differential circuits have required the application and measurement of voltages and currents, which is difficult at RF and microwave frequencies. Scattering parameters ( $s$ -parameters) have been developed for characterization and analysis at these frequencies [3], but have been applied primarily to single-ended circuits. A modification of existing  $s$ -parameter techniques is needed to measure differential-mode and common-mode circuit performance at microwave frequencies.

Currently, it is possible to measure common-mode  $s$ -parameters on wafer with standard ground-signal-ground probes to more than 100 GHz [4]. However, a differential circuit requires a balanced probe to launch differential signals. A balanced probe provided by Cascade Microtech [5] allows some characterization of differential signals with addition of

180 degree splitter/combiners. However, these probes attenuate the common-mode signal, so that it is neglected, although typically non-zero. Testing with separate differential probes and common-mode probes will allow for more complete  $s$ -parameter characterization of differential circuits, but until this work, there has been little examination of this subject.

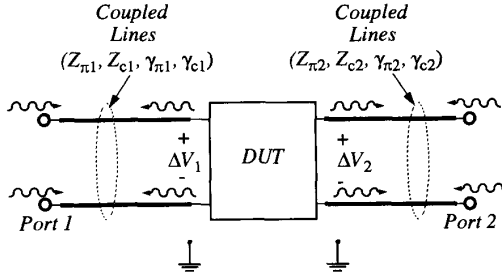
A severe limitation in differential-mode/common-mode circuit characterization is a lack of applicable power wave and  $s$ -parameter theory. There is no reported way (known to the authors) to describe  $s$ -parameters based on mixed differential-mode/common-mode propagation. Previous work most closely related to this work has been specific to descriptions of coupled transmission lines [6]–[14] and shielded balanced transmission lines. Work by the National Bureau of Standards on balanced transmission lines uses  $s$ -parameters to describe differential-mode propagation, but neglects common-mode propagation and any mode conversions [15]. In the literature, the coupled transmission work has been most commonly applied to directional couplers [16]–[19] with Cohn and Levy [20] providing a historical perspective on the role of coupled transmission lines in directional coupler development. Past work on coupled transmission lines has largely focused on voltage/current relationships and Z, Y, and ABCD-parameter descriptions of TEM circuits. One notable exception to the Z/Y/ABCD-parameter approach is work by Krage and Haddad [21] which employs traditional normalized power waves to describe coupler behavior. However, all of the referenced work deals with specific TEM structures, and is not suitable for characterization of a generic differential circuit. The present paper provides the theory behind the mixed propagation mode based  $s$ -parameters suitable for general microwave differential circuit characterization, and demonstrates its utility with simulations on Hewlett-Packard's Microwave Design System (MDS) [22].

This paper is organized as follows: In Section II the Mixed-mode two-port circuit is presented, and the definition of the coupled line transmission system is given. Mixed-mode power waves and mixed-mode  $s$ -parameters are developed in Section III. Section IV discusses special considerations necessary for mixed-mode measurement systems. Section V presents the ideal mixed-mode two-port measurement system and simulations using MDS. Finally, conclusions are presented in the last Section VI.

## II. MIXED-MODE TWO-PORT CIRCUIT

The concept of a microwave differential circuit is examined in this section. In a practical RF/microwave implementation,

Manuscript received July 25, 1994; revised December 23, 1994.  
D. E. Bockelman is with the Motorola Radio Products Applied Research, Plantation, FL 33322 USA.  
W. R. Eisenstadt is with the University of Florida, Gainesville, FL 32611 USA.  
IEEE Log Number 9412044.

Fig. 1. Schematic of differential  $s$ -parameter measurement.

such a differential circuit is based on pairs of coupled transmission lines. A schematic of a typical two-port RF/microwave differential system is shown in Fig. 1. Essential features of the microwave differential circuit in Fig. 1 are the coupled pair transmission line input and output. It is conceptually beneficial to define a signal that propagates between the lines of the coupled-pair (as opposed to propagating between one line and ground). Such signals are known as differential signals, and can be described by a difference of voltage ( $\Delta V_1 \neq 0, \Delta V_2 \neq 0$ ) and current flow between the individual lines in a pair. By such a definition, the signal is not referenced to a ground potential, but rather the signal on one line of the coupled pair is referenced to the other. Further, this differential signal should propagate in a TEM, or quasi-TEM, fashion with a well-defined characteristic impedance and propagation constant. Coupled line pairs, as in Fig. 1, allow propagating differential signals (the quantities of interest) to exist. The differential circuit discussion in this paper will be limited to the two-port case, but the generalized theory for  $n$ -port circuits can be readily derived from this work.

Most practical implementations of Fig. 1 will incorporate a ground plane, or some other global reference conductor, either intentionally or unintentionally. This ground plane allows another mode of propagation to exist, namely common-mode propagation. Conceptually, the common-mode wave applies equal signals with respect to ground at each of the individual lines in a coupled pair, such that the differential voltage is zero (i.e.  $\Delta V_1 = \Delta V_2 = 0$ ). The ability of the microwave differential circuit to propagate both common-mode and differential-mode signals requires any complete theoretical treatment to include characterization of all simultaneously propagating modes. For convenience, the simultaneous propagation of two or more modes (namely, differential-mode, and common-mode) on a coupled transmission line will be referred to in this paper as mixed-mode propagation, from which mixed-mode  $s$ -parameters will be defined.

### III. MIXED-MODE POWER WAVES AND $S$ -PARAMETERS

To begin the presentation of mixed-mode  $s$ -parameters, a general asymmetric coupled transmission line pair over a ground plane will be analyzed. This analysis yields multiple propagating modes all referenced to ground. These modes will be used to express the desired differential signal between the lines of the coupled-pair, as well as the common signal

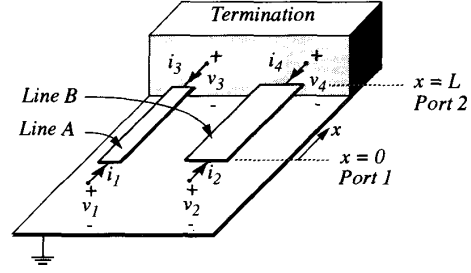


Fig. 2. Schematic of asymmetric coupled-pair transmission lines.

referenced to ground. Fig. 2 is a diagram of such a coupled-pair transmission line, with all pertinent voltages and currents denoted. Also shown in Fig. 2 is a representation of a termination for the coupled-pair line. Later, this paper will use these lines as reference lines at the input and output of an arbitrary DUT. Subject to the simplifying assumptions, the mathematical results of this paper are applicable to any pair of conductors with a nearby ground conductor.

Referring again to Fig. 2, the behavior of the coupled-line pair can be described by [6]

$$\begin{aligned} -\frac{dv_1}{dx} &= z_1 i_1 + z_m i_2 \\ -\frac{dv_2}{dx} &= z_2 i_2 + z_m i_1 \\ -\frac{di_1}{dx} &= y_1 v_1 + y_m v_2 \\ -\frac{di_2}{dx} &= y_2 v_2 + y_m v_1 \end{aligned} \quad (1)$$

where  $z_1$  and  $z_2$  are self-impedances per unit length,  $y_1$  and  $y_2$  are admittances per unit length, and  $z_m$  and  $y_m$  are mutual impedance and admittance per unit length, respectively. Also, a harmonic time dependence (i.e.  $e^{j\omega t}$ ) is assumed.

The solution to the set of (1) as published by Tripathi [6] is given as

$$\begin{aligned} v_1 &= A_1 e^{-\gamma_c x} + A_2 e^{\gamma_c x} + A_3 e^{-\gamma_\pi x} + A_4 e^{\gamma_\pi x} \\ v_2 &= A_1 R_c e^{-\gamma_c x} + A_2 R_c e^{\gamma_c x} + A_3 R_\pi e^{-\gamma_\pi x} + A_4 R_\pi e^{\gamma_\pi x} \\ i_1 &= \frac{A_1}{Z_{c1}} e^{-\gamma_c x} - \frac{A_2}{Z_{c2}} e^{\gamma_c x} + \frac{A_3}{Z_{\pi 1}} e^{-\gamma_\pi x} - \frac{A_4}{Z_{\pi 2}} e^{\gamma_\pi x} \\ i_2 &= \frac{A_1 R_c}{Z_{c1}} e^{-\gamma_c x} - \frac{A_2 R_c}{Z_{c2}} e^{\gamma_c x} + \frac{A_3 R_\pi}{Z_{\pi 1}} e^{-\gamma_\pi x} - \frac{A_4 R_\pi}{Z_{\pi 2}} e^{\gamma_\pi x} \end{aligned} \quad (2)$$

where  $A_1$ , and  $A_3$  represent the phasor coefficients for the forward (positive  $x$ ) propagating  $c$  and  $\pi$ -modes, respectively, and  $A_2$ , and  $A_4$  represent the phasor coefficients for the reverse (negative  $x$ ) propagating  $c$  and  $\pi$ -modes, respectively. The characteristic impedance of the  $c$ -modes are represented by  $Z_{c1}$  and  $Z_{c2}$  for lines A and B, respectively, and the characteristic impedance of the  $\pi$ -modes are represented by  $Z_{\pi 1}$  and  $Z_{\pi 2}$  for lines A and B, respectively. Additionally,  $R_c = v_2/v_1$  for  $\gamma = \pm\gamma_c$ ,  $R_\pi = v_2/v_1$  for  $\gamma = \pm\gamma_\pi$ , and

$$\begin{aligned} \gamma_{c,\pi}^2 &= \frac{y_1 z_1 + y_2 z_2}{2} + y_m z_m \pm \frac{1}{2} [(y_1 z_1 - y_2 z_2)^2 \\ &\quad + 4(z_1 y_m + y_2 z_m)(z_2 y_m + y_1 z_m)]^{1/2}. \end{aligned} \quad (3)$$

Each voltage/current pair at each node represent a single propagating signal referenced to the ground potential. These signals will be called nodal waves.

A practical simplification in the development of mixed-mode  $s$ -parameter theory is to assume symmetric coupled pairs (i.e., lines A and B have equal width) as reference transmission lines. This assumption allows simple mathematical formulations of mixed-mode  $s$ -parameters. Furthermore, this assumption is not overly limiting, since reference lines may be made arbitrarily short. For symmetrical lines, in (2)  $R_c = 1$  and  $R_\pi = -1$ , and the  $c$  and the  $\pi$ -modes become the *even* and *odd* modes, respectively, as first used by Cohn [13]. For notational purposes, we shall use the substitutions  $c \rightarrow e$  and  $\pi \rightarrow o$  for even-mode and odd-mode, respectively. With these substitutions, the mode characteristic impedances and propagation constants become

$$\begin{aligned} Z_{c1} &= Z_{c2} = Z_e \\ Z_{\pi 1} &= Z_{\pi 2} = Z_o \\ \gamma_c &= \gamma_e \quad \gamma_\pi = \gamma_o. \end{aligned} \quad (4)$$

Expressing (2) in the symmetric case

$$\begin{aligned} v_1 &= A_1 e^{-\gamma_e x} + A_2 e^{\gamma_e x} + A_3 e^{\gamma_o x} + A_4 e^{-\gamma_o x} \\ v_2 &= A_1 e^{-\gamma_e x} + A_2 e^{\gamma_e x} - A_3 e^{-\gamma_o x} - A_4 e^{\gamma_o x} \\ i_1 &= \frac{A_1}{Z_e} e^{-\gamma_e x} - \frac{A_2}{Z_e} e^{\gamma_e x} + \frac{A_3}{Z_o} e^{-\gamma_o x} - \frac{A_4}{Z_o} e^{\gamma_o x} \\ i_2 &= \frac{A_1}{Z_e} e^{-\gamma_e x} - \frac{A_2}{Z_e} e^{\gamma_e x} - \frac{A_3}{Z_o} e^{-\gamma_o x} + \frac{A_4}{Z_o} e^{\gamma_o x}. \end{aligned} \quad (5)$$

As before, these voltage/current pairs are nodal waves at each terminal that are referenced to ground.

It is important, now, to define the differential and common-mode voltages and currents to develop a self-consistent set of mixed-mode  $s$ -parameters. Define the differential-mode voltage at a point,  $x$ , to be the difference of between voltages on node 1 and node 2

$$v_{dm}(x) \equiv v_1 - v_2. \quad (6)$$

This standard definition establishes a signal that is no longer referenced to ground. In a differential circuit, one would expect equal current magnitudes to enter the positive input terminal as leaves the negative input terminal. Therefore, the differential-mode current is defined as one-half the difference between currents entering nodes 1 and 2

$$i_{dm}(x) \equiv \frac{1}{2}(i_1 - i_2). \quad (7)$$

Definitions in (6) and (7) are self-consistent with the differential power delivered to a differential load. These definitions differ from previously published definitions by Zysman and Johnson [10] due to change in references. The common-mode voltage in a differential circuit is typically the average voltage at a port. Hence, common-mode voltage is one half the sum of the voltages on nodes 1 and 2

$$v_{cm}(x) \equiv \frac{1}{2}(v_1 + v_2). \quad (8)$$

The common-mode current at a port is simply the total current flowing into the port. Therefore, define the common-mode current as the sum of the currents entering nodes 1 and 2

$$i_{cm}(x) \equiv i_1 + i_2. \quad (9)$$

Note: The return current for the common-mode signal flows through the ground plane. Again, these definitions differ from definitions from Zysman and Johnson [10] due to change in references.

Expressing these differential and common-mode values (6) through (9) in terms of the line voltages and currents (5)

$$\begin{aligned} v_{dm}(x) &= 2(A_3 e^{-\gamma_o x} + A_4 e^{\gamma_o x}) \\ i_{dm}(x) &= \frac{A_3}{Z_o} e^{-\gamma_o x} - \frac{A_4}{Z_o} e^{\gamma_o x} \\ v_{cm}(x) &= A_1 e^{-\gamma_e x} + A_2 e^{\gamma_e x} \\ i_{cm}(x) &= 2\left(\frac{A_1}{Z_e} e^{-\gamma_e x} - \frac{A_2}{Z_e} e^{\gamma_e x}\right). \end{aligned} \quad (10)$$

Recall that  $A_1$  and  $A_2$  are the forward and reverse phasor coefficient for the even-mode propagation, and  $A_3$  and  $A_4$  are the forward and reverse phasor coefficient for the odd-mode propagation. If a short hand notation is introduced, a better understanding of these definitions can be had. Let

$$\begin{aligned} v_o^{\text{pos}}(x) &\equiv A_3 e^{-\gamma_o x} & v_o^{\text{neg}}(x) &\equiv A_4 e^{\gamma_o x} \\ v_e^{\text{pos}}(x) &\equiv A_1 e^{-\gamma_e x} & v_e^{\text{neg}}(x) &\equiv A_2 e^{\gamma_e x} \\ i_o^{\text{pos}}(x) &\equiv \frac{A_3}{Z_o} e^{-\gamma_o x} & i_o^{\text{neg}}(x) &\equiv \frac{A_4}{Z_o} e^{\gamma_o x} \\ i_e^{\text{pos}}(x) &\equiv \frac{A_1}{Z_e} e^{-\gamma_e x} & i_e^{\text{neg}}(x) &\equiv \frac{A_2}{Z_e} e^{\gamma_e x}. \end{aligned} \quad (11)$$

Then (5) becomes

$$\begin{aligned} v_1 &= v_e^{\text{pos}}(x) + v_e^{\text{neg}}(x) + v_o^{\text{pos}}(x) + v_o^{\text{neg}}(x) \\ v_2 &= v_e^{\text{pos}}(x) + v_e^{\text{neg}}(x) - v_o^{\text{pos}}(x) - v_o^{\text{neg}}(x) \\ i_1 &= i_e^{\text{pos}}(x) - i_e^{\text{neg}}(x) + i_o^{\text{pos}}(x) - i_o^{\text{neg}}(x) \\ i_2 &= i_e^{\text{pos}}(x) - i_e^{\text{neg}}(x) - i_o^{\text{pos}}(x) + i_o^{\text{neg}}(x) \end{aligned} \quad (12)$$

and (10) becomes

$$\begin{aligned} v_{dm}(x) &= 2(v_o^{\text{pos}}(x) + v_o^{\text{neg}}(x)) \\ i_{dm}(x) &= i_o^{\text{pos}}(x) - i_o^{\text{neg}}(x) = \frac{v_o^{\text{pos}}(x) - v_o^{\text{neg}}(x)}{Z_o} \\ v_{cm}(x) &= v_e^{\text{pos}}(x) + v_e^{\text{neg}}(x) \\ i_{cm}(x) &= 2(i_e^{\text{pos}}(x) - i_e^{\text{neg}}(x)) = 2\frac{v_e^{\text{pos}}(x) - v_e^{\text{neg}}(x)}{Z_e}. \end{aligned} \quad (13)$$

Note that, in general,  $Z_o \neq Z_e$ .

Characteristic impedances of each mode can be defined as the ratio of the voltage to current of the appropriate modes at any point,  $x$ , along the line. These impedances can be expressed in terms of the even and odd-mode (ground referenced) characteristic impedances

$$Z_{dm} \equiv \frac{v_{dm}^{\text{pos}}(x)}{i_{dm}^{\text{pos}}(x)} = \frac{2v_o^{\text{pos}}(x)}{v_o^{\text{pos}}(x)/Z_o} = 2Z_o \quad (14)$$

$$Z_{cm} \equiv \frac{v_{cm}^{\text{pos}}(x)}{i_{cm}^{\text{pos}}(x)} = \frac{v_e^{\text{pos}}(x)}{(2v_e^{\text{pos}}(x))/Z_e} = \frac{Z_e}{2}. \quad (15)$$

These relations between the even/odd mode characteristic impedances and the differential/common mode characteristic impedances are consistent with the matched load terminations discussed in the literature [7], [8].

Now that voltages, currents, and characteristic impedances have been defined for both differential and common modes, the normalized power waves can be developed. By the definition for a generalized power wave at the  $n$ th port [23], [24]

$$\begin{aligned} a_n &= \frac{1}{2\sqrt{\text{Re}(Z_n)}} [v_n + i_n Z_n] \\ b_n &= \frac{1}{2\sqrt{\text{Re}(Z_n)}} [v_n - i_n Z_n^*] \end{aligned} \quad (16)$$

where  $a_n$  is the normalized wave propagating in the forward (positive  $x$ ) direction,  $b_n$  is the normalized wave propagating in the reverse (negative  $x$ ) direction, and  $Z_n$  is the characteristic impedance of the port. With the above definitions, the differential normalized waves become, at port 1

$$\begin{aligned} a_{dm1} &\equiv a_{dm}(0) = \frac{1}{2\sqrt{\text{Re}(Z_{dm})}} [v_{dm}(x) + i_{dm}(x)Z_{dm}]|_{x=0} \\ b_{dm1} &\equiv b_{dm}(0) = \frac{1}{2\sqrt{\text{Re}(Z_{dm})}} [v_{dm}(x) - i_{dm}(x)Z_{dm}^*]|_{x=0}. \end{aligned} \quad (17)$$

Similarly, define the common-mode normalized waves, at port 1, as

$$\begin{aligned} a_{cm1} &\equiv a_{cm}(0) = \frac{1}{2\sqrt{\text{Re}(Z_{cm})}} [v_{cm}(x) + i_{cm}(x)Z_{cm}]|_{x=0} \\ b_{cm1} &\equiv b_{cm}(0) = \frac{1}{2\sqrt{\text{Re}(Z_{cm})}} [v_{cm}(x) - i_{cm}(x)Z_{cm}^*]|_{x=0}. \end{aligned} \quad (18)$$

Analogous definitions at port 2 can easily be found by setting  $x = l$ .

Imposing the condition of low-loss transmission lines on the coupled-pair of Fig. 2, the characteristic impedances are approximately purely real [24]. Under this restriction,  $Z_{dm} \approx \text{Re}\{Z_{dm}\} \equiv R_{dm}$  and  $Z_{cm} \approx \text{Re}\{Z_{cm}\} \equiv R_{cm}$ . With this assumption, the normalized wave equations at port 1 can be simplified

$$\begin{aligned} a_{dm1} &= \frac{1}{2\sqrt{R_{dm}}} [v_{dm}(x) + i_{dm}(x)R_{dm}]|_{x=0} \\ b_{dm1} &= \frac{1}{2\sqrt{R_{dm}}} [v_{dm}(x) - i_{dm}(x)R_{dm}]|_{x=0} \\ a_{cm1} &= \frac{1}{2\sqrt{R_{cm}}} [v_{cm}(x) + i_{cm}(x)R_{cm}]|_{x=0} \\ b_{cm1} &= \frac{1}{2\sqrt{R_{cm}}} [v_{cm}(x) - i_{cm}(x)R_{cm}]|_{x=0}. \end{aligned} \quad (19)$$

With the normalized power waves defined, the development of mixed-mode  $s$ -parameters is straight forward. The definition of generalized  $s$ -parameters [23], [24] is

$$[\mathbf{b}] = [\mathbf{S}][\mathbf{a}] \quad (21)$$

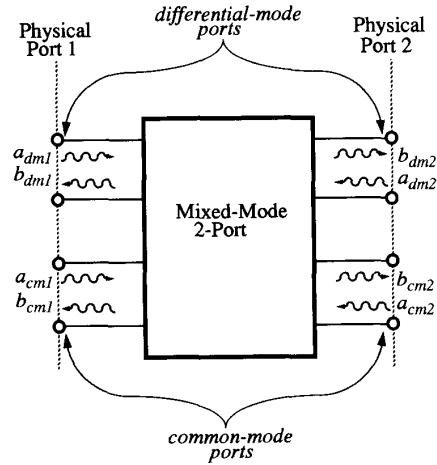


Fig. 3. Conceptual diagram of mixed-mode two-port.

where the bold letters denote an  $n$ -dimensional column vector or an  $n$ -by- $n$  matrix. Given a coupled-line two-port like Fig. 2, or any arbitrary mixed-mode two-port, the generalized mixed-mode  $s$ -parameters can be given as

$$\begin{aligned} b_{dm1} &= s_{11}a_{dm1} + s_{12}a_{dm2} + s_{13}a_{cm1} + s_{14}a_{cm2} \\ b_{dm2} &= s_{21}a_{dm1} + s_{22}a_{dm2} + s_{23}a_{cm1} + s_{24}a_{cm2} \\ b_{cm1} &= s_{31}a_{dm1} + s_{32}a_{dm2} + s_{33}a_{cm1} + s_{34}a_{cm2} \\ b_{cm2} &= s_{41}a_{dm1} + s_{42}a_{dm2} + s_{43}a_{cm1} + s_{44}a_{cm2} \end{aligned} \quad (22)$$

where the subscripts 1 and 2 denote ports 1 and 2, respectively. Here,  $[\mathbf{S}]$  can be described by

$$\begin{bmatrix} b_{dm1} \\ b_{dm2} \\ b_{cm1} \\ b_{cm2} \end{bmatrix} = \begin{bmatrix} \mathbf{S}_{dd} & \mathbf{S}_{dc} \\ \mathbf{S}_{cd} & \mathbf{S}_{cc} \end{bmatrix} \begin{bmatrix} a_{dm1} \\ a_{dm2} \\ a_{cm1} \\ a_{cm2} \end{bmatrix}. \quad (23)$$

The following names are used: Call  $[\mathbf{S}_{dd}]$  the differential  $s$ -parameters,  $[\mathbf{S}_{cc}]$  the common-mode  $s$ -parameters, and  $[\mathbf{S}_{dc}]$  and  $[\mathbf{S}_{cd}]$  the mode-conversion or cross-mode  $s$ -parameters. In particular,  $[\mathbf{S}_{dc}]$  describes the conversion of common-mode waves into differential-mode waves, and  $[\mathbf{S}_{cd}]$  describes the conversion of differential-mode waves into common-mode waves. These four partitions are analogues to four transfer gains ( $A_{cc}, A_{dd}, A_{cd}, A_{dc}$ ) introduced by Middlebrook [2].

These mixed-mode two-port  $s$ -parameters can be shown graphically (see Fig. 3) as a traditional four-port. It must be remembered, however, that the ports are conceptual tools only, and not physically separate ports.

#### IV. CONSIDERATIONS FOR A PRACTICAL MIXED-MODE MEASUREMENT SYSTEM

The most straightforward means of implementing a mixed-mode  $s$ -parameter measurement system is to directly apply differential and common-mode waves while measuring the resulting differential and common-mode waves. Unfor-

tunately, the generation and measurement of these modes of propagation is not easily achievable with standard vector network analyzers (VNA). However, under certain conditions, one can relate the total nodal waves (each representing two modes of propagation) to the desired differential and common-mode waves. These nodal waves are readily generated and measured with standard VNAs, and with consideration, the differential and common-mode waves, and hence the mixed-mode  $s$ -parameters, can be calculated. Therefore, the relationships between the normalized mixed-mode waves ( $a_{dm1}, b_{dm1}, a_{cm1}, b_{cm1}$ , etc.) and the nodal waves ( $a_1, b_1, a_2, b_2$ , etc.) will be derived, and the necessary conditions for these relationships to exist will be found.

If one is to make a general purpose RF measurement port, the values of characteristic port impedances must be chosen. It is useful to require the even and odd-mode characteristic impedances of the measurement system to be equal, thus reducing the number of different valued matched terminations required. In contrast, it is difficult to fabricate lumped termination standards for coupled lines where  $Z_e$  does not equal  $Z_o$ . If the characteristic impedances of the lines are defined to be equal (say,  $50 \Omega$ ), then a further simplification of the above expressions can be accomplished with the substitution  $Z_e = Z_o = Z_0$  where in the low-loss case  $Z_0 \approx \text{Re}\{Z_0\} \equiv R_0$ .

By choosing equal even and odd-mode characteristic impedances, one is selecting a special case of coupled transmission line behavior, as described in (1). Enforcing equal even and odd-mode characteristic impedances is equivalent to the conditions of uncoupled transmission lines. As has been shown in the literature [7], the condition  $Z_e = Z_o$  results in the mutual impedances and admittances being zero ( $z_m = 0, y_m = 0$ ). Under these conditions, the describing differential equations of the transmission line system (1) clearly become uncoupled, resulting in two independent transmission line solutions. Although very specific, this is a valid solution to (1), and all results up to this point are also valid under the special case of equal even and odd-mode characteristic impedances. Therefore, we choose the reference lines of the mixed-mode  $s$ -parameters to be uncoupled transmission lines. The key to this choice is that these uncoupled reference lines can be easily interfaced with a coupled line system, as discussed below.

To interpret the meaning of uncoupled reference transmission lines, consider a system of transmission lines: one coupled pair, and one uncoupled pair connected in series with the coupled pair. If even and odd (or  $c$  and  $\pi$ ) modes are both propagating (forward and reverse) on the coupled pair, then it can be shown that the waves propagating on each of the uncoupled transmission lines are linear combinations of the waves propagating on the coupled system (see Appendix). Furthermore, the differential and common-mode normalized waves of the coupled pair system can be reconstructed from the normalized waves at a point on the uncoupled line pairs (see Appendix). This point of reconstruction is arbitrary, and one may choose the point to be the interface between the coupled system and the uncoupled reference lines.

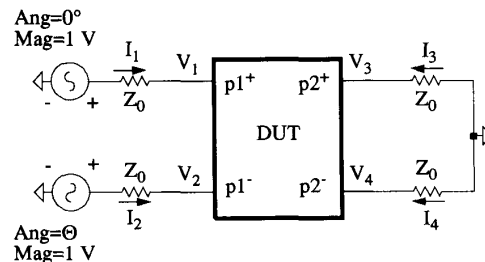


Fig. 4. Conceptual diagram of mixed-mode two-port measurement system.

Substituting  $Z_e = Z_o = Z_0 \approx R_0$ , the normalized nodal waves of the coupled lines at the interface are

$$\begin{aligned} a_i &= \frac{1}{2\sqrt{R_0}}[v_i + i_i R_0] \\ b_i &= \frac{1}{2\sqrt{R_0}}[v_i - i_i R_0] \end{aligned} \quad (24)$$

where  $a_i$  and  $b_i$  are the normalized forward and reverse propagating nodal waves at node  $i$ , respectively, and  $i \in \{1, 2, 3, 4\}$ . These equations are applicable only in the case of low-loss lines, with equal even and odd mode characteristic impedance. By combining (12), (19), (20) and (24), it can be shown that the differential and common-mode waves at port 1 are

$$\begin{aligned} a_{dm1} &= \frac{1}{\sqrt{2}}(a_1 - a_2)|_{x=0} & a_{cm1} &= \frac{1}{\sqrt{2}}(a_1 + a_2)|_{x=0} \\ b_{dm1} &= \frac{1}{\sqrt{2}}(b_1 - b_2)|_{x=0} & b_{cm1} &= \frac{1}{\sqrt{2}}(b_1 + b_2)|_{x=0}. \end{aligned} \quad (25)$$

Similarly, for port 2

$$\begin{aligned} a_{dm2} &= \frac{1}{\sqrt{2}}(a_3 - a_4)|_{x=l} & a_{cm2} &= \frac{1}{\sqrt{2}}(a_3 + a_4)|_{x=l} \\ b_{dm2} &= \frac{1}{\sqrt{2}}(b_3 - b_4)|_{x=l} & b_{cm2} &= \frac{1}{\sqrt{2}}(b_3 + b_4)|_{x=l}. \end{aligned} \quad (26)$$

Equations (25) and (26) represent important relationships from which mixed-mode  $s$ -parameters can be determined with a practical measurement system. To understand the utility of the above relationships, consider Fig. 4, which is a conceptual model for a mixed-mode measurement system. By adjusting the phase difference,  $\Theta$ , between the two sources to  $0^\circ$  or  $180^\circ$  one can determine the common-mode or differential-mode forward  $s$ -parameters, respectively. Conceptually, the measured quantities are the voltages and currents. These values can be related to the normalized nodal waves,  $a_1, b_1, a_2, b_2$ , etc., through the generalized definitions given in (24). From these nodal waves, the differential and common-mode normalized waves, and hence, the mixed-mode  $s$ -parameters, can be calculated. Physically, the various ratios of nodal waves,  $a_1, b_1, a_2, b_2$ , etc., are measured, and from these ratios the mixed-mode  $s$ -parameters are found.

The physical implementation of a mixed-mode  $s$ -parameter measurement system can be achieved with a modification of a standard VNA. The differential stimulus of a coupled two-port requires the input waves at the reference plane

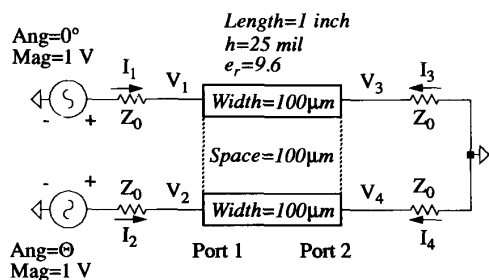


Fig. 5. Schematic of mixed-mode  $s$ -parameter simulation of symmetric coupled-pair transmission line.

to be  $180^\circ$  apart. One possible way this can be achieved through a single signal source is with the use of a  $180^\circ$ -3-dB-hybrid splitter/combiner. The construction of the differential reflected and transmitted waves can be also completed through a  $180^\circ$  splitter/combiner. The common-mode stimulus of a coupled two-port requires the input waves at the reference plane to be  $0^\circ$  apart. This can also be achieved through a single signal source with the use of a  $0^\circ$ -3-dB-hybrid splitter/combiner, with the construction of the common-mode reflected and transmitted waves also completed through a  $0^\circ$  splitter/combiner.

The calibration of such a system can be achieved through the extension of VNA calibration theory. Detailed calibration discussion is beyond the scope of this paper, but will be the subject of future work. It is interesting to note, however, that any successful calibration algorithm must correct both magnitude and phase imbalances in the splitter/combiners and signal paths, since any such imbalances will represent errors in the generation and reconstruction of the mixed-mode waves. Also, any calibration will be greatly assisted by requiring one standard for both  $Z_e$  and  $Z_o$ , which is accomplished when  $Z_e = Z_o$ , as assumed in this section.

All mixed-mode normalized waves and  $s$ -parameters have been discussed with respect to a transmission pair line as a reference. Conceptually, this reference line must be attached to every port of a DUT. However, there is no restriction on the length of these reference lines. Therefore, the reference lines can be of zero length, and the definitions of all mixed-mode quantities will still apply, with one provision. Namely, the generator source impedance and the load impedances must match the characteristic impedance of the reference lines. The use of zero length reference lines is a useful interpretation of the general normalized wave definition of (24) from which the mixed-mode  $s$ -parameters are defined.

It is interesting to note that an alternative requirement can be found through which the nodal and mixed-mode waves

can be related. One could require the differential-mode and common-mode characteristic impedances to be equal (i.e.  $Z_{dm} = Z_{cm} = Z_0$ ). The relationships (25) and (26) will change, however. This alternate requirement may have value in some cases, but the original requirement ( $Z_e = Z_o = Z_0$ ) best relates mixed-mode  $s$ -parameters to standard  $s$ -parameters.

## V. IDEAL MIXED-MODE MEASUREMENT SYSTEM AND SIMULATIONS

Equations (25) and (26) form the basis of an ideal mixed-mode  $s$ -parameter measurement system. These equations can be implemented into a microwave simulator, and can provide a quick and simple method of illustrating the usefulness of mixed-mode  $s$ -parameters.

The circuit in Fig. 4 was implemented into Hewlett-Packard's MDS. The phase difference,  $\Theta$ , between the two sources was set to  $0^\circ$  for the common-mode and common-to-differential-mode forward  $s$ -parameters. For the forward differential-mode and differential-to-common-mode  $s$ -parameters, the phase difference was set to  $180^\circ$ . In each case, the nodal waves were calculated from (25), (26), and (24), and the  $s$ -parameters were calculated with the appropriate ratios. The reverse  $s$ -parameters were calculated by driving port 2 of the DUT with  $50 \Omega$  loads at port 1.

The first example of mixed-mode  $s$ -parameters uses a DUT that is pair of coupled microstrip transmission lines, with symmetric (i.e. equal width) top conductors. This symmetric coupled-pair, and the accompanying circuitry, is shown in Fig. 5. Each runner width is  $100 \mu\text{m}$  with an edge-to-edge spacing of  $100 \mu\text{m}$ . The substrate is 25-mil-thick alumina with a relative permittivity of 9.6 with a loss tangent of 0.001, and the metal conductivity is that of copper,  $\sim 5.8 \times 10^7 \text{ S/m}$ . A one inch section of this line was simulated in MDS as described above, and the mixed-mode  $s$ -parameters at 5 GHz are shown in (27) at the bottom of this page.

As expected, each partitioned sub-matrix demonstrates the properties of a reciprocal, passive and (port) symmetric DUT. The differential  $s$ -parameters,  $S_{dd}$ , show the coupled pair possesses an odd-mode characteristic impedance of  $50 \Omega$  ( $100\text{-}\Omega$ -differential impedance), and has low-loss propagation in the differential mode. The common-mode  $s$ -parameters,  $S_{cc}$ , show the coupled pair possesses an even-mode characteristic impedance other than  $50 \Omega$ . Actually, the even-mode impedance of the pair is  $140 \Omega$  ( $70\text{-}\Omega$  common-mode impedance). Note the cross-mode  $s$ -parameters are zero for the symmetric coupled pair indicating no conversion between propagation modes.

The second example is similar to the first, except the coupled microstrip transmission lines are asymmetric (i.e. unequal widths). This asymmetric coupled-pair, and the accompanying

$$\begin{bmatrix} S_{dd} & S_{dc} \\ S_{cd} & S_{cc} \end{bmatrix} = \begin{bmatrix} 0.001\angle-141^\circ & 0.972\angle9.53^\circ & 0 & 0 \\ 0.972\angle9.53^\circ & 0.001\angle-141^\circ & 0 & 0 \\ 0 & 0 & 0.341\angle-60.4^\circ & 0.915\angle-26.4^\circ \\ 0 & 0 & 0.915\angle-26.4^\circ & 0.341\angle-60.4^\circ \end{bmatrix} \quad (27)$$

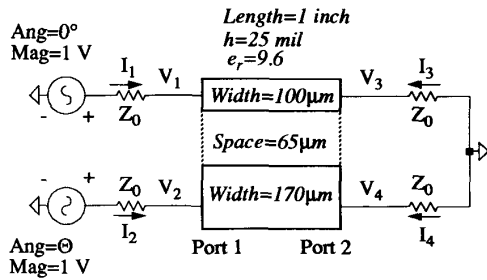


Fig. 6. Schematic of mixed-mode simulation of asymmetric coupled-pair transmission line.

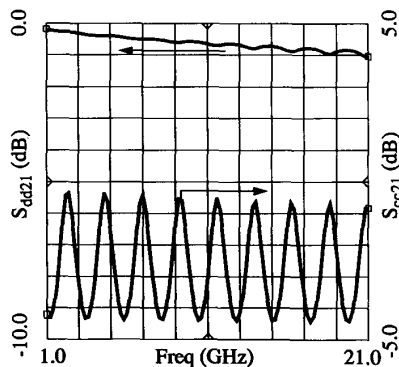


Fig. 7. Simulated magnitude in dB of  $S_{dd21}$  and  $S_{cc21}$  versus frequency for asymmetric coupled-pair line.

circuitry, is shown in Fig. 6. One top conductor width is  $100 \mu\text{m}$ , and the second is  $170 \mu\text{m}$ , with an edge-to-edge spacing of  $65 \mu\text{m}$ . Again, the substrate is 25-mil-thick alumina with a relative permittivity of 9.6 with a loss tangent of 0.001, and the metal conductivity is that of copper. A one inch section of this line was simulated in MDS at 5 GHz, and the mixed-mode  $s$ -parameters are shown in (28) at the bottom of the page.

As in the first example, each partitioned sub-matrix demonstrates the properties of a reciprocal, passive and (port) symmetric DUT. Also like the first example, the differential  $s$ -parameters show the coupled pair possesses an odd-mode characteristic impedance of nearly  $50 \Omega$  (actually  $49 \Omega$ ), and has low-loss propagation in the differential mode. The common-mode  $s$ -parameters show the coupled pair has a greater degree of mismatch than the first example (the even-mode impedance is  $152 \Omega$  in this case).

The most important difference between the two examples is seen in the cross-mode  $s$ -parameters. The data in (28)

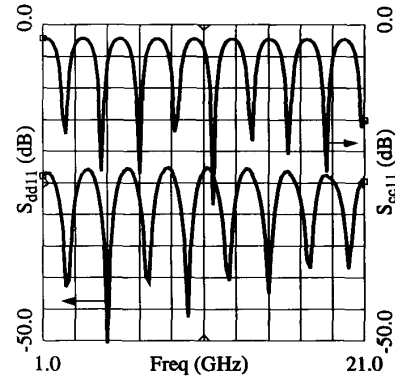


Fig. 8. Simulated magnitude in dB of  $S_{dd11}$  and  $S_{cc11}$  versus frequency for asymmetric coupled-pair line.

shows significant conversion between propagation modes, particularly in transmission parameters  $S_{dc21}$  and  $S_{cd21}$ . Note these two sub-matrices are equal indicating equal conversion from differential to common-mode and from common to differential-mode. These non-zero  $s$ -parameters can be interpreted conceptually in the following way. In the case of  $S_{cd21}$ , a pure differential mode wave is impinging on port 1 of the DUT. However, at port 2, both differential and common-mode waves exist. Some of the energy of the differential wave is converted to a common-mode propagation, and the total energy is preserved (except for losses in the metal and dielectric).

This example circuit was simulated across frequency, and the magnitudes of selected mixed-mode  $s$ -parameters are plotted in Figs. 7–10. Fig. 7 shows both  $S_{dd21}$  and  $S_{cc21}$  in dB from 1–21 GHz. The ripple pattern across frequency in the common-mode transmission ( $S_{cc21}$ ) indicates an impedance mismatch at the ports for common-mode propagation. At the higher frequencies of the plot, the finite conductivity of the conductors is evident as average loss increases. The differential-mode transmission ( $S_{dd21}$ ) shows smaller ripples (0.2-dB maximum), indicating smaller mismatch, and also shows lower average loss. However, the losses due to the reflections at the ports do not account for all of the ripple in the differential transmission. As can be seen in Fig. 8, the return loss for the differential mode is greater than 20 dB, which can account for approximately 0.04 dB of worst case loss (over ohmic losses). Mode conversion accounts for the remaining reduction in the differential-mode, and hence  $S_{dd21}$  is reduced. Here, differential energy is converted to both common-mode transmission  $S_{cd21}$  and common-mode reflection  $S_{cd11}$ . Fig. 9 shows the cross-mode transmission  $S_{cd21}$  in dB, and Fig. 10 shows the cross-mode reflection  $S_{cd11}$  in dB. The minima in

$$\begin{bmatrix} S_{dd} & S_{dc} \\ S_{cd} & S_{cc} \end{bmatrix} = \begin{bmatrix} 0.003 \angle -175^\circ & 0.956 \angle 1.819^\circ & 0.005 \angle -177^\circ & 0.031 \angle 80.7^\circ \\ 0.956 \angle 1.819^\circ & 0.003 \angle -175^\circ & 0.031 \angle 80.7^\circ & 0.005 \angle -177^\circ \\ 0.005 \angle -177^\circ & 0.031 \angle 80.7^\circ & 0.502 \angle 48.0^\circ & 0.844 \angle -40.2^\circ \\ 0.031 \angle 80.7^\circ & 0.005 \angle -177^\circ & 0.844 \angle -40.2^\circ & 0.502 \angle -48.0^\circ \end{bmatrix}. \quad (28)$$

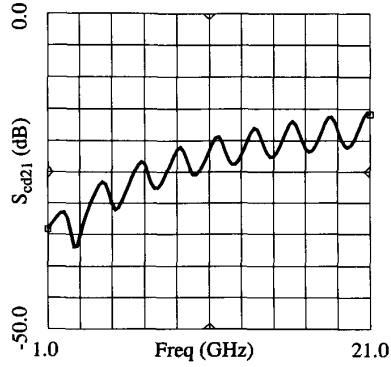


Fig. 9. Simulated magnitude in dB of  $S_{cd21}$  versus frequency for asymmetric coupled-pair line.

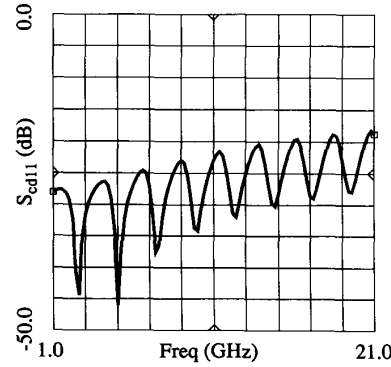


Fig. 10. Simulated magnitude in dB of  $S_{cd11}$  versus frequency for asymmetric coupled-pair line.

the differential-mode transmission  $S_{dd21}$  correspond to a worst case point in the relative phases of  $S_{dd21}$ ,  $S_{cd21}$ , and  $S_{cd11}$ . In a low loss transmission line case, the insertion loss due to mode conversion and miss-match can be shown to be approximately

$$\text{Loss (dB)} \approx -10 \log[1 - (|S_{dd11}|^2 + |S_{cd21}|^2 + |S_{cd11}|^2)]. \quad (29)$$

This is consistent with the increasing ripple in  $S_{dd21}$  with increasing frequency since the mode conversion ( $S_{cd21}$  and  $S_{cd11}$ ) increases with frequency.

## VI. CONCLUSION

A theory for mixed-mode  $s$ -parameters is developed for characterization of microwave differential circuits. The theory is based on microwave coupled line systems, and is useful to describe general differential circuits, including coupled transmission lines. The theory is applied to develop the concept of an ideal mixed-mode  $s$ -parameter measurement system, and the restriction of equal even and odd-mode characteristic impedances is shown to result in useful relationships for such a system. A real mixed-mode measurement system can be implemented from the results of this theoretical work. However, a proper mathematical basis is needed in the future

for characterization and calibration of these measurements. Finally, microwave simulations illustrate some of the utility of mixed-mode  $s$ -parameters.

## APPENDIX TRANSMISSION OF MODES FROM COUPLED TO UNCOUPLED LINES

Consider a system where a pair of coupled transmission lines are connected in cascade with a pair of uncoupled transmission lines, as shown in Fig. A-1. The coupled pair will be considered to be a reference line as defined in Section III; hence, the coupled pair line is symmetric and low loss. The normalized waves at the outputs of the uncoupled lines will be investigated under the same assumptions, namely low loss and symmetry, which for the uncoupled case means the lines are identical. The voltages at a point  $x$  on the coupled pair lines are given by (12), rewritten here to explicitly show the complex exponentials

$$\begin{aligned} v_1(x) &= V_e^{\text{pos}} e^{-\gamma_e x} + V_e^{\text{neg}} e^{\gamma_e x} + V_o^{\text{pos}} e^{-\gamma_o x} + V_o^{\text{neg}} e^{\gamma_o x} \\ v_2(x) &= V_e^{\text{pos}} e^{-\gamma_e x} + V_e^{\text{neg}} e^{\gamma_e x} - V_o^{\text{pos}} e^{-\gamma_o x} - V_o^{\text{neg}} e^{\gamma_o x} \end{aligned} \quad (\text{A-1})$$

and the currents, also given by (12) are

$$\begin{aligned} i_1(x) &= \frac{V_e^{\text{pos}}}{Z_e} e^{-\gamma_e x} - \frac{V_e^{\text{neg}}}{Z_e} e^{\gamma_e x} + \frac{V_o^{\text{pos}}}{Z_o} e^{-\gamma_o x} - \frac{V_o^{\text{neg}}}{Z_o} e^{\gamma_o x} \\ i_2(x) &= \frac{V_e^{\text{pos}}}{Z_e} e^{-\gamma_e x} - \frac{V_e^{\text{neg}}}{Z_e} e^{\gamma_e x} - \frac{V_o^{\text{pos}}}{Z_o} e^{-\gamma_o x} + \frac{V_o^{\text{neg}}}{Z_o} e^{\gamma_o x}. \end{aligned} \quad (\text{A-2})$$

With the uncoupled transmission lines, the voltages and currents at a point  $x$  are

$$\begin{aligned} v_{ui}(x) &= V_{ui}^{\text{pos}} e^{-\gamma_u x} + V_{ui}^{\text{neg}} e^{\gamma_u x} \\ i_{ui}(x) &= \frac{V_{ui}^{\text{pos}}}{Z_u} e^{-\gamma_u x} - \frac{V_{ui}^{\text{neg}}}{Z_u} e^{\gamma_u x} \end{aligned} \quad (\text{A-3})$$

with  $i = 1, 2$  and  $Z_{u1} = Z_{u2} = Z_u$ ,  $\gamma_{u1} = \gamma_{u2} = \gamma_u$ . At the interface between the coupled pair and the uncoupled pair, ( $x = 0, x' = d$ ) the voltages and currents of the two systems must conform to the boundary conditions

$$\begin{aligned} v_{u1}(0) &= v_1(0) & i_{u1}(0) &= i_1(0) \\ v_{u2}(0) &= v_2(0) & i_{u2}(0) &= i_2(0). \end{aligned} \quad (\text{A-4})$$

Through the application of these boundary conditions and (A-1)–(A-3), the phasor coefficients on the uncoupled lines are found to be

$$\begin{aligned} V_{u1}^{\text{pos}} &= \frac{1}{2} \left[ V_e^{\text{pos}} \left( 1 + \frac{Z_u}{Z_e} \right) + V_e^{\text{neg}} \left( 1 - \frac{Z_u}{Z_e} \right) \right. \\ &\quad \left. + V_o^{\text{pos}} \left( 1 + \frac{Z_u}{Z_o} \right) + V_o^{\text{neg}} \left( 1 - \frac{Z_u}{Z_o} \right) \right] \\ V_{u1}^{\text{neg}} &= \frac{1}{2} \left[ V_e^{\text{pos}} \left( 1 - \frac{Z_u}{Z_e} \right) + V_e^{\text{neg}} \left( 1 + \frac{Z_u}{Z_e} \right) \right. \\ &\quad \left. + V_o^{\text{pos}} \left( 1 - \frac{Z_u}{Z_o} \right) + V_o^{\text{neg}} \left( 1 + \frac{Z_u}{Z_o} \right) \right] \end{aligned} \quad (\text{A-5})$$

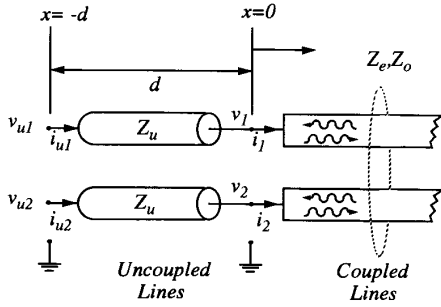


Fig. A-1. Schematic of uncoupled pair in cascade with coupled pair-line.

$$\begin{aligned}
 V_{u2}^{\text{pos}} &= \frac{1}{2} \left[ V_e^{\text{pos}} \left( 1 + \frac{Z_u}{Z_e} \right) + V_e^{\text{neg}} \left( 1 - \frac{Z_u}{Z_e} \right) \right. \\
 &\quad \left. - V_o^{\text{pos}} \left( 1 + \frac{Z_u}{Z_o} \right) - V_o^{\text{neg}} \left( 1 - \frac{Z_u}{Z_o} \right) \right] \\
 V_{u2}^{\text{neg}} &= \frac{1}{2} \left[ V_e^{\text{pos}} \left( 1 - \frac{Z_u}{Z_e} \right) + V_e^{\text{neg}} \left( 1 + \frac{Z_u}{Z_e} \right) \right. \\
 &\quad \left. - V_o^{\text{pos}} \left( 1 - \frac{Z_u}{Z_o} \right) - V_o^{\text{neg}} \left( 1 + \frac{Z_u}{Z_o} \right) \right]. \quad (\text{A-6})
 \end{aligned}$$

The differential-mode voltage at the output of the uncoupled pair ( $x = -d$ ) can be defined by (6) as

$$v_{\text{dm}_u}(-d) = v_{u1}(-d) - v_{u2}(-d) \quad (\text{A-7})$$

which can be found to be

$$v_{\text{dm}_u}(-d) = V_{\text{dm}_u}^{\text{pos}} e^{\gamma_u d} + V_{\text{dm}_u}^{\text{neg}} e^{-\gamma_u d} \quad (\text{A-8})$$

where

$$V_{\text{dm}_u}^{\text{pos}} = V_{u1}^{\text{pos}} - V_{u2}^{\text{pos}} \quad V_{\text{dm}_u}^{\text{neg}} = V_{u1}^{\text{neg}} - V_{u2}^{\text{neg}}. \quad (\text{A-9})$$

The normalized forward differential-mode wave at the output of the coupled pair, defined generally by (16), can be shown as

$$a_{\text{dm}_u} = \frac{V_{\text{dm}_u}^{\text{pos}}}{\sqrt{R_{\text{dm}_u}}} \quad (\text{A-10})$$

where  $R_{\text{dm}_u}$  is the (approximately) purely real characteristic impedance of the differential-mode, defined between the uncoupled lines, and  $R_{\text{dm}_u} = 2R_u$  where  $R_u$  is the characteristic impedance of the each of the uncoupled lines. From (A-5), (A-6), (A-9) and (A-10), it is found that

$$\begin{aligned}
 a_{\text{dm}_u} &= \frac{1}{2} \sqrt{\frac{R_{\text{dm}}}{R_{\text{dm}_u}}} \left[ a_{\text{dm}} \left( 1 + \frac{R_{\text{dm}_u}}{R_{\text{dm}}} \right) \right. \\
 &\quad \left. + b_{\text{dm}} \left( 1 - \frac{R_{\text{dm}_u}}{R_{\text{dm}}} \right) \right] e^{j\beta_u d} \quad (\text{A-11})
 \end{aligned}$$

where  $a_{\text{dm}}$  and  $b_{\text{dm}}$  is the differential-mode normalized forward and reverse waves of the coupled system at  $x = 0$ , and  $R_{\text{dm}}$  is the approximately real characteristic impedance of the differential-mode on the coupled-pair. Similarly, the

remaining differential and common-mode normalized waves can be shown to be

$$\begin{aligned}
 b_{\text{dm}_u} &= \frac{1}{2} \sqrt{\frac{R_{\text{dm}}}{R_{\text{dm}_u}}} \left[ b_{\text{dm}} \left( 1 + \frac{R_{\text{dm}_u}}{R_{\text{dm}}} \right) \right. \\
 &\quad \left. + a_{\text{dm}} \left( 1 - \frac{R_{\text{dm}_u}}{R_{\text{dm}}} \right) \right] e^{-j\beta_u d} \\
 a_{\text{cm}_u} &= \frac{1}{2} \sqrt{\frac{R_{\text{cm}}}{R_{\text{cm}_u}}} \left[ a_{\text{cm}} \left( 1 + \frac{R_{\text{cm}_u}}{R_{\text{cm}}} \right) \right. \\
 &\quad \left. + b_{\text{cm}} \left( 1 - \frac{R_{\text{cm}_u}}{R_{\text{cm}}} \right) \right] e^{j\beta_u d} \\
 b_{\text{cm}_u} &= \frac{1}{2} \sqrt{\frac{R_{\text{cm}}}{R_{\text{cm}_u}}} \left[ b_{\text{cm}} \left( 1 + \frac{R_{\text{cm}_u}}{R_{\text{cm}}} \right) \right. \\
 &\quad \left. + a_{\text{cm}} \left( 1 - \frac{R_{\text{cm}_u}}{R_{\text{cm}}} \right) \right] e^{-j\beta_u d} \quad (\text{A-12})
 \end{aligned}$$

where  $b_{\text{dm}}$ ,  $a_{\text{cm}}$ , and  $b_{\text{cm}}$  are the normalized waves of the coupled system at  $x = 0$ . Therefore, the differential and common-mode normalized waves at the output of the uncoupled lines are equal to the corresponding coupled system waves with a phase-shift and a scaling factor due to the different characteristic impedances. To the resulting mixed-mode  $s$ -parameters, the phase-shift and the scaling factor represent an arbitrary reference plane shift and a re-normalization to the characteristic impedance of the uncoupled transmission lines, respectively. Because of this, the coupled pair reference line can be replaced with an uncoupled pair reference, and the resulting mixed-mode  $s$ -parameters are simply transposed to a different reference impedance by the uncoupled lines. Therefore, the mixed-mode  $s$ -parameters of an arbitrary  $n$ -port DUT can be measured with  $n$  pairs of uncoupled transmission lines.

## REFERENCES

- [1] P. R. Gray and R. G. Meyer, *Analysis and Design of Analog Integrated Circuits*, 3rd ed. New York: Wiley, 1993.
- [2] R. D. Middlebrook, *Differential Amplifiers*. New York: Wiley, 1963.
- [3] T. T. Ha, *Solid-State Microwave Amplifier Design*, reprint ed. Malabar, FL: Krieger, 1991.
- [4] *Application Note: WPH-505/805 Waveguide-Input Wafer Probes*. Beaverton, OR: Cascade Microtech, 1993.
- [5] D. E. Carlton *et al.*, "Microwave wafer probing," *Microwave J.*, vol. 29, pp. 121-129, Jan. 1985.
- [6] V. K. Tripathi, "Asymmetric coupled transmission lines in an inhomogeneous medium," *IEEE Trans. Microwave Theory Tech.*, vol. MTT-23, pp. 734-739, Sept. 1975.
- [7] K. D. Marx, "Propagation modes, equivalent circuits, and characteristic terminations for multiconductor transmission lines with inhomogeneous dielectrics," *IEEE Trans. Microwave Theory Tech.*, vol. MTT-21, pp. 450-457, Nov. 1973.
- [8] H. Amemiya, "Time-domain analysis of multiple parallel transmission lines," *RCA Rev.*, vol. 28, pp. 241-276, June 1967.
- [9] R. A. Speciale and V. K. Tripathi, "Wave-modes and parameter matrices of non-symmetrical coupled lines in a non-homogeneous medium," *Int. J. Electron.*, vol. 40, pp. 371-375, Apr. 1976.
- [10] G. I. Zysman and A. K. Johnson, "Coupled transmission line networks in an inhomogeneous dielectric medium," *IEEE Trans. Microwave Theory Tech.*, vol. MTT-17, pp. 753-759, Oct. 1969.
- [11] E. G. Vlostovskiy, "Theory of coupled transmission lines," *Telecommun. Radio Eng.*, vol. 21, pp. 87-93, Apr. 1967.
- [12] S. B. Cohn, "Characteristic impedances of broadside-coupled strip transmission lines," *IRE Trans. Microwave Theory Tech.*, vol. MTT-10, pp. 633-637, Nov. 1960.

- [13] S. B. Cohn, "Shielded coupled-strip transmission lines," *IRE Trans. Microwave Theory Tech.*, vol. MTT-5, pp. 29-38, Oct. 1955.
- [14] R. A. Speciale, "Fundamental even- and odd-mode waves for nonsymmetrical coupled lines in non-homogeneous media," in *1974 IEEE MTT Int. Microwave Symp. Dig. Tech. Papers*, June 1974, pp. 156-158.
- [15] W. L. Gans and N. S. Nahman, "Shielded balanced and coaxial transmission lines—Parametric measurements and instrumentation relevant to signal waveform transmission in digital service," NBS Tech. Note 1042, National Bureau of Standards, June 1981.
- [16] C. Tsai and K. C. Gupta, "A generalized model for coupled lines and its applications to two-layer planar circuits," *IEEE Trans. Microwave Theory Tech.*, vol. MTT-40, pp. 2190-2199, Dec. 1992.
- [17] C. B. Sharpe, "An equivalence principle for nonuniform transmission line directional couplers," *IEEE Trans. Microwave Theory Tech.*, vol. MTT-15, pp. 398-405, July 1967.
- [18] E. M. T. Jones and J. T. Bolljahn, "Coupled-strip-transmission-line filters and directional couplers," *IRE Trans. Microwave Theory Tech.*, vol. MTT-4, pp. 75-81, Apr. 1956.
- [19] B. M. Oliver, "Directional electromagnetic couplers," *Proc. IRE*, vol. 42, pp. 1686-1692, Nov. 1954.
- [20] S. B. Cohn and R. Levy, "History of microwave passive components with particular attention to directional couplers," *IEEE Trans. Microwave Theory Tech.*, vol. MTT-32, pp. 1046-1054, July 1984.
- [21] M. K. Krage and G. I. Haddad, "Characteristics of coupled microstrip transmission lines—I: Coupled-mode formation of inhomogeneous dielectrics," *IEEE Trans. Microwave Theory Tech.*, vol. MTT-18, pp. 217-222, Nov. 1970.
- [22] *HP 85150B Microwave and RF Design Systems: User Documentation*. Santa Rosa, CA: Hewlett-Packard, 1992.
- [23] K. Kurokawa, "Power waves and the scattering matrix," *IEEE Trans. Microwave Theory Tech.*, vol. MTT-13, pp. 194-202, Mar. 1965.
- [24] G. Gonzalez, *Microwave Transistor Amplifiers*. Englewood Cliffs, NJ: Prentice-Hall, 1984.



**David E. Bockelman** (S'88-M'90) received the B.S. and M.S. degrees in electrical engineering from the Georgia Institute of Technology, Atlanta, Georgia, in 1989 and 1990, respectively. He is pursuing the Ph.D. in electrical engineering at the University of Florida, Gainesville, FL.

He joined the Applied Research Department of Motorola Radio Products Group in 1990, where he is currently a senior engineer. His work has included microwave device characterization and modeling, and active device noise measurement. His current

interests include distortion theory, nonlinear modeling, and microwave circuit design.



**William R. Eisenstadt** (S'78-M'84-SM'92) received the B.S., M.S., and Ph.D. degrees in electrical engineering from Stanford University, Stanford, CA, in 1979, 1981, and 1986, respectively.

In 1984, he joined the faculty of the University of Florida, Gainesville, FL, where he is now an Associate Professor. His research is concerned with high-frequency characterization, simulation and modeling of integrated circuit devices, packages, and interconnect. In addition, he is interested in large-signal microwave circuit design.

Dr. Eisenstadt received the NSF Presidential Young Investigator Award in 1985.